Catalysis Today xxx (2013) xxx–xxx

Contents lists available at SciVerse ScienceDirect

Catalysis Today

journal homepage: www.elsevier.com/locate/cattod

Graphical Abstract

Catalysis Today xxx (2013) xxx–xxx

Solar ~~photo-fenton~~ optimization for the treatment of MWTP effluents containing emerging contaminants

L. Prieto-Rodríguez, D. Spasiano, I. Oller*, I. Fernández-Calderero, A. Agüera, S. Malato

In this study, solar photo-Fenton process is proposed and optimized as a tertiary treatment for MWTP effluents containing emerging contaminants (ECs) and other micro-pollutants. A three-level factorial experimental design (~~3~~3), modified with 2 × 3 axial and 6 central runs to make it spherical was carried out for optimization using Statgraphics software. The influence of hydrogen peroxide dosage, iron (II) concentration and temperature were assessed over accumulated energy (~~QUV~~Q_{UV} kJ/L as the response factor) necessary to remove more than 95% of the micro-pollutants. Finally, the optimal operating conditions were successfully applied to the treatment of a real MWTP effluent reaching complete ECs removal after 3.47 kJ/L.

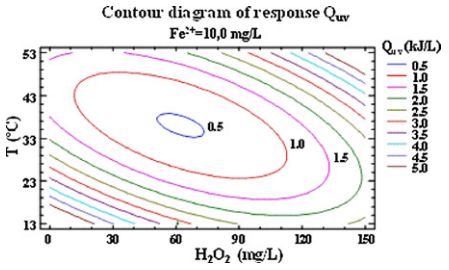

Catalysis Today xxx (2013) xxx–xxx

Contents lists available at SciVerse ScienceDirect

Catalysis Today

journal homepage: www.elsevier.com/locate/cattod

Highlights

Catalysis Today xxx (2013) xxx–xxx

Solar ~~photo-fenton~~ optimization for the treatment of MWTP effluents containing emerging contaminants

L. Prieto-Rodríguez, D. Spasiano, I. Oller*, I. Fernández-Calderero, A. Agüera, S. Malato

- Solar photo-Fenton tertiary treatment is optimized for micro-pollutants elimination.
- HPLC-QTRAP-MS was employed for monitoring micro-contaminants removal.
- Spherical factorial experimental design with 2×3 axial and 6 central runs was used.
- Q_{UV} mostly influenced by iron concentration, temperature, and their interaction.
- Optimal operating conditions were tested on a real MWTP effluent ($Q_{UV} < 4$ kJ/L).

Catalysis Today xxx (2013) xxx–xxx

Contents lists available at SciVerse ScienceDirect

Catalysis Today

journal homepage: www.elsevier.com/locate/cattod

Solar photo-~~fenton~~ optimization for the treatment of MWTP effluents containing emerging contaminants

Q1 L. Prieto-Rodríguez[a], D. Spasiano[c], I. Oller[a,*], I. Fernández-Calderero[a], A. Agüera[b], S. Malato[a]

Q2 [a] Plataforma Solar de Almería-CIEMAT, Solar Treatment of Water Research Group, Carretera de Senés Km 4, 04200 Tabernas, Almería, Spain
[b] Pesticide Residue Research Group, University of Almería, 04120 Almería, Spain
[c] Department of Chemical Engineering, Faculty of Engineering, University of Naples Federico II, P.le V. Tecchio, 80, 80125 Naples, Italy

ARTICLE INFO

Article history:
Received 1 July 2012
Received in revised form 8 January 2013
Accepted 15 January 2013
Available online xxx

Keywords:
Experimental design
Micro-pollutants
Solar photo-Fenton
Tertiary treatment

ABSTRACT

Growing use of xenobiotic substances, synthetic fragrances, pesticides, drugs, and other contaminants is leading to their increasing concentrations in the aquatic environment (over 1 μg/L). Conventional municipal wastewater treatment plants (MWTP) are unable to degrade these contaminants entirely. In this study, solar photo-Fenton process is proposed and optimized as a tertiary treatment for MWTP effluents containing emerging contaminants (ECs) and other micro-pollutants. A three-level factorial experimental design (3^3), modified with 2×3 axial and 6 central runs to make it spherical was carried out for optimization using Statgraphics software. The influence of hydrogen peroxide dosage, iron (II) concentration and temperature were assessed over accumulated energy (Q_{UV} kJ/L as the response factor) necessary to remove more than 95% of the micro-pollutants. Pareto graphic and response surfaces showed that Fe (II) concentration, temperature and their interaction are the variables that influence the response factor the most. Finally, the optimal operating conditions were successfully applied to the treatment of a real MWTP effluent at pilot plant scale removing 80% of total micropollutants after 0.56 kJ/L.

1. Introduction

One of the main environmental objectives of the EC Water Framework Directive (WFD), Article 4, is to achieve and maintain "good status" of all community waters including inland surface and ground waters, transitional and coastal waters by 2015 [1]. Detection of many new compounds in surface water, groundwater and drinking water in recent years raises considerable public concern in this sense, especially when guidelines based on human health are unavailable [2]. Some of the nearly 300 million tons of synthetic compounds annually used in industrial and consumer products partially find their way into natural waters. This is especially true of frequently used pharmaceuticals and personal care products (PPCPs), which are continually introduced in the aquatic environment through sewage treatment plants or directly released from the skin during swimming or bathing [3,4]. One important class of such contaminants posing an increasing threat to aquatic organisms, as well as to human health, is made up of the endocrine disrupting compounds (EDCs). EDCs include naturally occurring estrogens, synthetic estrogens, phyto-estrogens and xeno-estrogens (e.g., pesticides, plasticizers, persistent organochlorines, organohalogens, alkyl phenols, and heavy metals) [5].

The limited effectiveness of conventional municipal wastewater treatment plants (MWTPs) for removing such chemicals, which are only partially removed by biological and/or adsorption processes, has been widely demonstrated [6,7]. Therefore, a wide array of trace pollutants, defined as low concentrations of an environmental contaminant, normally in the nanogram (ng) or microgram per liter (μg/L) range, escape treatment, becoming ubiquitous contaminants in the environment [8,9]. So this group of micro-pollutants must be removed before MWTP effluents are discharged into the environment, as a multitude of risks, such as bacterial resistance, sterility, and feminization of aquatic organisms derive from the presence of these substances in water [10,11].

In recent years, intensive efforts have been made to develop efficient technologies for the removal of persistent micro-contaminants from aqueous matrices. Detoxification of effluent streams containing polar and hydrophilic chemicals by advanced oxidation processes (AOPs) such as photocatalysis [12–14], ozone technologies [15–17] and ultrasound oxidation [18,19] have been recently under study. However, this application is still commercially unavailable because of the associated high operating costs, including electricity demand for ozonation, electrochemical-oxidations and UV lamps [20]. That is why research in AOPs which can be driven by solar radiation is receiving more attention. Some papers have reported on the application of photo-Fenton in

* Corresponding author. Tel.: +34 950387993; fax: +34 950365015.
E-mail address: isabel.oller@psa.es (I. Oller).

0920-5861/$ – see front matter © 2013 Elsevier B.V. All rights reserved.
http://dx.doi.org/10.1016/j.cattod.2013.01.002

particular as a tertiary treatment to remove micro-pollutants at relatively low concentrations (ng/L–μg/L) [21,22]. In addition, it is highly important to consider that degradation of contaminants (usually contained in industrial wastewater) with conventional photo-Fenton (iron in the mM range) is not the best choice for eliminating micro-pollutants present in MWTP effluents at extremely low concentrations, because an additional treatment step would be required to manage the large amount of iron mud resulting from final catalyst precipitation. Although results presented in such publications were rather satisfactory, it became essential to optimize the operating parameters in order to make commercial applications feasible.

In photo-Fenton, the Fenton reagent produces OH• radicals when H_2O_2 is added to Fe^{2+} salts. The organic pollutant degradation rate is strongly accelerated by irradiation with UV–vis light [23]. Under these conditions, photolysis of Fe^{3+} complexes promotes Fe^{2+} regeneration, and iron may be considered a true catalyst (Eqs. (1)–(3)).

$$Fe^{2+} + H_2O_2 \rightarrow Fe^{3+} + OH^- + OH^\bullet \quad (1)$$

$$Fe^{3+} + H_2O + h\nu \rightarrow Fe^{2+} + H^+ + OH^\bullet \quad (2)$$

$$[Fe^{3+}L_n] + h\nu \rightarrow [Fe^{2+}L_{n-1}] + L_{ox}^\bullet \quad (3)$$

One factor considerably affecting cost is oxidant reagent consumption [24]. Hydrogen peroxide can be rate-limiting if applied in concentrations that are too low. On the contrary, in a concentration which is too high, it can compete with contaminants for the hydroxyl radicals generated (Eq. (4)), and also self-decompose into oxygen and water (Eq. (5)).

$$OH^\bullet + H_2O_2 \rightarrow H_2O + OH_2^\bullet \quad (4)$$

$$H_2O_2 \rightarrow H_2O + (1/2)O_2 \quad (5)$$

The operating parameters to be optimized in the photo-Fenton tertiary treatment of MWTP effluents containing micro-pollutants are: temperature, and catalyst (iron salt) and hydrogen peroxide concentrations. In solar-driven systems, as the most important investment cost is the CPC field, the final objective must be minimizing the accumulated UV energy required for contaminants completely degradation. Furthermore, it is widely known that temperature control is highly important, as increasing temperature always has a beneficial effect on reactions kinetics until certain value when the process efficiency begins to low [25,26]. Experimental design methodology has been widely used for photo-Fenton optimization in different applications [27,28]. Nevertheless, as far as we know this methodology has not been used for the optimization of solar photo-Fenton tertiary treatment of a real MWTP effluent, containing micropollutants in the range of concentrations of ng/L, yet.

Accordingly, this study was based on an experimental design for optimization of the solar photo-Fenton tertiary treatment of real MWTP effluents from El Ejido (Almería, Spain) spiked with 100 μg/L of four micropollutants (2-Hyroxy Phenil, Progesterone, Carbamazepine and Flumequine) monitored by UPLC-UV. The accumulated energy needed to remove over 95% of the contaminant load was selected as the response factor that had to be minimized. The Statgraphics Software Statistical tool was employed to analyze the experimental results and to plot the corresponding response surfaces.

Finally, the optimal operating conditions found by Statgraphics software were successfully applied to a real MWTP effluent in which 46 micropollutants were detected and quantified (overall concentration higher than 40 μg/L).

2. Materials and methods

2.1. Reagents and real wastewater

Photo-Fenton experiments were performed using iron sulphate ($FeSO_4 \cdot 7H_2O$). Sulfuric acid used to strip HCO_3^-/CO_3^{2-} (and for lowering pH < 3, optimal value for photo-Fenton process) and hydrogen peroxide (30%, w/v) were purchased from Panreac. All reagents used for chromatographic analyses, and ultrapure (Milli-Q) water, were HPLC grade. Analytical standards of progesterone, flumequine, carbamazepine, and 2-hydroxy-biphenyl for chromatography analyses and for experiments were purchased from Sigma–Aldrich. The same real MWTP effluent taken downstream from the secondary biological treatment of the El Ejido MWTP (in the Province of Almería, Spain) was used in all the experiments. Dissolved organic carbon (DOC), total inorganic carbon (TIC) and chemical oxygen demand (COD) were 10.2, 105 and 23 mg/L, respectively. Other characteristics of the effluent were, in mg/L: Cl^- 43, SO_4^{2-} 24, NO_3^- 1.9, Na^+ 35, K^+ 4.1, Ca^{+2} 12, Mg^{+2} 8.9, and NH_4^+ 3.2.

2.2. Analytical procedures

Dissolved organic carbon and total inorganic carbon were measured immediately by a Shimadzu TOC-VCSN analyzer. Total iron concentration was monitored by colorimetric determination with 1,10-phenanthroline according to ISO 6332, using a Unicam-2 spectrophotometer. Hydrogen peroxide concentration was analyzed in the laboratory by a spectrophotometric method at 410 nm based on the formation of a yellow complex from the reaction of titanium (IV) oxysulfate with H_2O_2 following DIN 38409 H15.

The concentration of the four emerging contaminants was monitored by ultra-performance liquid chromatography (flow rate: 1 mL min^{-1}) (Agilent Technologies, series 1200) with a UV-DAD detector and a C-18 analytical column (Agilent XDB-C18, 1.8 μm, 4.6 mm × 50 mm, 600 bar). The mobile phase was 10% UPLC-grade acetonitrile and 90% water with formic acid 25 mM. Detection was done at three different wavelengths depending on the compound: 267 nm (Carbamazepine), 248 nm (Flumequine and progesterone), and 243 nm (2-hydroxy-biphenyl). For UPLC analyses 10 mL of sample were passed through a 0.22-μm syringe filter, then 1 mL of UPLC-grade acetonitrile was also passed through the filter to extract any compound adsorbed on the filter.

The concentration profile of each compound during degradation of micropollutants present in effluents in the nanogram range was determined by LC–MS analysis. A solid-phase extraction (SPE) procedure [29] was applied using commercial Oasis HLB (divinylbenzene/N-vinylpyrrolidone copolymer) cartridges (200 mg, 6 cm^3). The ASPEC GX-271, an automated sample processor used was equipped with a 406 Single Syringe pump and a VALVEMATE® II valve actuator, all provided by Gilson. The HPLC-QTRAP-MS method for target compound analysis [30] was developed for the 3200 QTRAP MS/MS system (Applied Biosystems, Concord, ON, Canada). Separation of the analytes was performed using an HPLC (series 1100, Agilent Technologies) equipped with a 250 mm long and 3.0 mm i.d. reversed-phase C-18 analytical column (Zorbax SB, Agilent Technologies). The analyses were carried out using a turbo ion spray source in positive and negative modes, and Applied Biosystems/MDS Sciex Analyst software for data acquisition and processing

2.3. Experimental setup

Photo-Fenton experiments were performed in a Compound Parabolic Collector (CPC) solar pilot plant specially developed for photo-Fenton applications and operated in batch recirculation

Please cite this article in press as: L. Prieto-Rodríguez, et al., Solar photo-fenton optimization for the treatment of MWTP effluents containing emerging contaminants, Catal. Today (2013), http://dx.doi.org/10.1016/j.cattod.2013.01.002

mode. The reactor loop consists of a continuously stirred tank, a centrifugal recirculation pump (1.5 m^3/h), compound parabolic collectors and connecting tubing and valves. The solar collector is composed of four 1.04 m^2 ~~compound parabolic collector (CPCs)~~ units [20] (total area of 4.16 m^2) with a concentration factor of 1, held by an aluminum profile frame mounted on a fixed platform tilted 37° and facing south. The total reactor volume is 75 L (V_T) and the total illuminated volume inside the absorber tubes is 44.6 L (V_i). The collectors were covered with special aluminum sheets for mixing in the dark. The temperature inside the reactor was kept constant during experiments using a temperature control system consisting of trace heating in the tubing, and a heat exchanger with a secondary water cooling cycle. An isometric map of this photo-Fenton solar reactor is available elsewhere [31].

Temperature, dissolved oxygen (DO) and pH in the pilot plant were measured online by the corresponding CRISON electrodes. Solar ultraviolet radiation (UV) was measured by a global UV radiometer (KIPP&ZONEN, model CUV3), mounted on a platform tilted 37° (the same angle as the CPCs). This gives an idea of the energy reaching any surface in the same position with respect to the sun.

The response factor considered in this study is the accumulated energy ~~Q~~ (kJ/L) necessary to remove over 95% of the ECs added as calculated by Eq. (6):

$$Q_{UV,n} = Q_{UV,n-1} + \Delta t_n \mathrm{UV} \frac{A_r}{V_T} \qquad (6)$$

$$\Delta t_n = t_n - t_{n-1}$$

where t_n is the experimental time for each sample, UV (kJ/L) is the average solar ultraviolet radiation measured during Δt_n and A_r is the collectors illuminated area (m^2). V_T (L) is the total volume of the pilot plant.

2.4. Experimental procedure

When received, the MWTP secondary biological treatment effluent was pretreated with H_2SO_4 under agitation to remove HCO_3^-/CO_3^{2-}, which are known to be hydroxyl radical scavengers [23,29]. Acid continued to be added until the pH reached the optimum for photo-Fenton process (pH < 3), ensuring elimination of HCO_3^-/CO_3^{2-}. In each one of the 32 experiments performed, 75 L of real MWTP effluent were spiked with 100 μg/L of four micro-pollutants: progesterone, flumequine, carbamazepine, and 2-hydroxy-biphenyl. After 30 min of homogenization, a sample was taken to assure initial contaminant concentration. Then the iron salt was added and homogenized in the dark for 20 more minutes. After that, the CPC solar reactor was uncovered, the hydrogen peroxide dose was added, and the experiment began. Samples were taken every 5 min for the first 30 min, and from then on, every 10 min until H_2O_2 was totally consumed, at which time the experiment ended.

In the experiment performed at optimal conditions with MWTP effluents with no added contaminants, samples were taken every 5 min and the reaction was immediately stopped for further analysis in LC–MS by removing residual H_2O_2 with catalase (2500 U/mg bovine liver, 100 mg/L) acquired from Fluka Chemie AG (Buchs, Switzerland) after adjusting the sample pH to 7.

2.5. Experimental design

This study evaluates the influence of some important parameters involved in the practical operation of solar photo-Fenton processes such as hydrogen peroxide dosage, iron concentration and temperature. A three-level factorial experimental design was employed to evaluate the influence of these three factors (H_2O_2, Fe^{2+} and T). The ranges used in this experimental design were 5–12 mg/L of Fe^{2+}, 40–100 mg/L of H_2O_2 and temperature from 20 to 40 °C. These are low concentrations of iron and hydrogen peroxide compared with industrial wastewater treatments, however in this case, the concentration of contaminants present in water is quite low.

Table 1
Experimental design matrix.

Runs	Block	Fe^{2+} (mg/L)	H_2O_2 (mg/L)	T (°C)
1	1	8.5	70	30
2	1	8.5	70	13.1
3	1	12	100	40
4	1	5	40	40
5	1	12	100	20
6	1	8.5	19.5	30
7	1	8.5	120.4	30
8	1	5	100	40
9	1	8.5	70	30
10	1	5	100	20
11	1	12	40	20
12	1	5	40	20
13	1	8.5	70	46.8
14	1	2.6	70	30
15	1	12	40	40
16	1	8.5	70	30
17	1	14.3	70	30
18	1	12	40	30
19	1	8.5	40	40
20	1	8.5	70	30
21	1	5	70	40
22	1	8.5	70	30
23	1	8.5	100	20
24	1	8.5	70	30
25	1	8.5	40	20
26	1	12	70	40
27	1	12	70	20
28	1	5	40	30
29	1	5	70	20
30	1	5	100	30
31	1	12	100	30
32	1	8.5	100	40

The three-level factorial experimental design (3^3) was modified to make it spherical with 2 × 3 axial and 6 central runs. The experimental design matrix (Table 1) summarizes the 32 runs which were performed. The Statgraphics statistical tool was employed to analyze the central composite design and to plot the response surfaces.

3. Results and discussions

Previous publications [22] have already reported on the elimination of very low concentrations of micro-contaminants by solar photo-Fenton, and studied the effect of different water matrices including real MWTP effluents. Nevertheless, the experimental parameters involved in the solar photo-Fenton process for the elimination of micro-pollutants, have never been optimized. The number of variables which affect this process is quite high: iron species and concentration, pH, temperature, irradiance intensity, contaminant concentration and characteristics, and water matrices. These parameters could significantly change depending on the nature of the wastewater to be treated [20]. This study has therefore selected an experimental design technique providing a systematic work method which allows conclusions to be drawn about the variables (or combination thereof) that significantly influence the response factor [32,33].

As mentioned above, the response factor was the accumulated energy necessary to remove over 95% of the micro-contaminants added to the real MWTP effluents. As the most important investment cost of a solar driven treatment facility is the CPC field, which

Please cite this article in press as: L. Prieto-Rodríguez, et al., Solar photo-fenton optimization for the treatment of MWTP effluents containing emerging contaminants, Catal. Today (2013), http://dx.doi.org/10.1016/j.cattod.2013.01.002

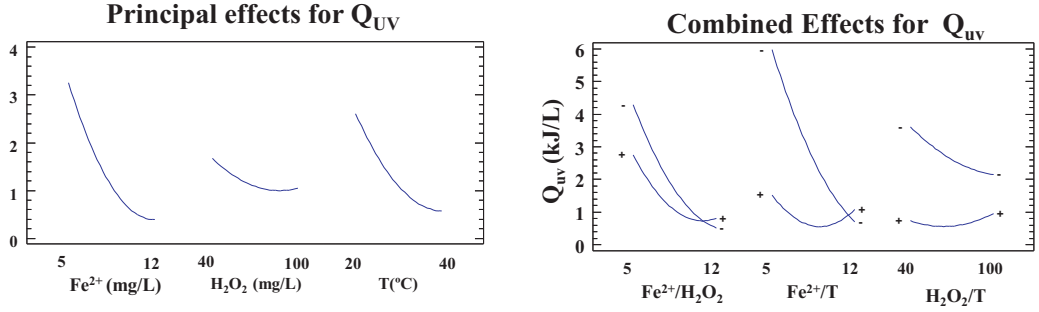

Fig. 1. (a) Main effect and (b) combined effect of each experimental parameter studied.

is directly related to the accumulated energy needed for complete elimination of the micro-pollutants, the main purpose of this study was to find the optimal operating parameters for minimizing the response factor.

The experimental design results in Fig. 1 show the effects of each parameter (Fe^{2+}, H_2O_2 and Temperature) on Q_{UV} separately and combined. Fig. 1(a) is plotted maintaining two of the three experimental parameters constant at their center points while following the third parameter separately. Fig. 1(b) shows the evolution of the combined effect of two of the three parameters at their highest (+) and the lowest (−) points while the third one is constant at its center point.

It is widely known that higher concentrations of iron increase the reaction rates, requiring less accumulated energy. In addition, higher temperatures also enhance reaction rates, reducing the Q_{UV} needed to an upper limit of around 45 °C at which process efficiency decreases due to catalyst precipitation, as previously observed by Zapata et al. [26]. This effect is clearly shown in Fig. 1(b). When the temperature was at its upper limit (40 °C) and the Fe^{2+} concentration was increasing from 5 to 12 mg/L, the accumulated energy required at first showed a decreasing profile and then started to increase very close to where the amount of catalyst is highest, decreasing process efficiency. Therefore, at higher temperatures, iron concentration presents an optimal.

The effect of hydrogen peroxide concentration (Fig. 1(a)) is not as dramatic as the effect of iron concentration. Although higher concentrations of H_2O_2 leads to lower Q_{UV}, an excess of this reagent (around 100 mg/L) did not significantly change the accumulated energy required. This means that high concentrations of H_2O_2 are not efficiently used in this kind of tertiary treatments, when the concentration of pollutants is so low and the treatment time expected is around tens of minutes. Indeed, considering the Fe^{2+}/H_2O_2 interaction (Fig. 1(b)), the same effect was observed, and at high Fe^{2+} and H_2O_2 concentrations, Q_{UV} remained almost constant, and accumulated energy was even better at lower hydrogen peroxide concentrations.

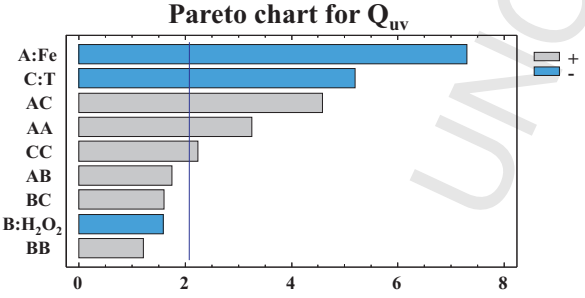

Fig. 2. Standardized Pareto Chart showing which of the variables and interactions studied are the most significant.

In Fig. 2 a Pareto chart is used to assist in deciding which of these variables and interactions are the most significant. This graph shows both the magnitude and importance of the effects (variables and interactions). The absolute value of the effects is displayed on the left vertical axis and the pseudo-error standard on the horizontal axis. The study was done for a 95% confidence interval. The vertical reference line, which corresponds to a simultaneous margin of error, means that any effect extending past this line is potentially important.

The Pareto chart confirms that the most significant effects are iron concentration and temperature, and their interactions. Furthermore, it should be stressed that the interactions between the variables alone are not beneficial for reducing the required Q_{UV}.

Eq. (7) fits the model of this experimental design with an R^2 of 0.85, which means that this model can explain 85% of the variability in Q_{UV}.

$$Q_{UV} = 33.04 - 2.77 \times Fe^{2+} - 0.132637 \times H_2O_2 - 0.795477 \times T + 0.06 \times Fe^{2+} + 0.004 \times Fe^{2+} \times H_2O_2 + 0.03 \times Fe^{2+} \times T + 0.0003 \times (H_2O_2)^2 + 0.00014 \times H_2O_2 \times T + 0.005 \times T^2 \quad (7)$$

Fe^{2+} and H_2O_2 are expressed in mg/L, and temperature (T) in °C.

3.1. Response surfaces for Q_{UV}

More detailed information on the strong dependence of the accumulated energy on Fe^{2+} concentration and temperature can be found from the corresponding response surfaces. The response surface graphs may be plotted using the experimental design results and Statgraphics statistical software. Fig. 3 shows four response surfaces for Q_{UV} versus temperature, hydrogen peroxide and iron concentration, while keeping one of the three variables constant in each plot.

The response surfaces in this study were selected based on the results of the operating parameters and their combination, which actually have a significant effect on the response factor in the experimental design.

Notice that in Fig. 3(a) at 5 mg/L of Fe^{2+} (the minimum studied in the experimental design), Q_{UV} was never below 1 kJ/L, even though it was always much lower at 12 mg/L of Fe^{2+} (maximum) (Fig. 3(b)). This shows that a catalyst concentration of 5 mg/L Fe^{2+} is too low catalyst concentration for carrying out the tertiary treatment of MWTP effluents. In addition, at 5 mg/L Fe^{2+}, the beneficial effect of temperature was stronger using less hydrogen peroxide, while Q_{UV} remains almost constant if temperature and H_2O_2 concentration increase (Fig. 3(a)).

Fig. 3(c) clearly shows the interaction between T and iron concentration on Q_{UV} when hydrogen peroxide concentration was

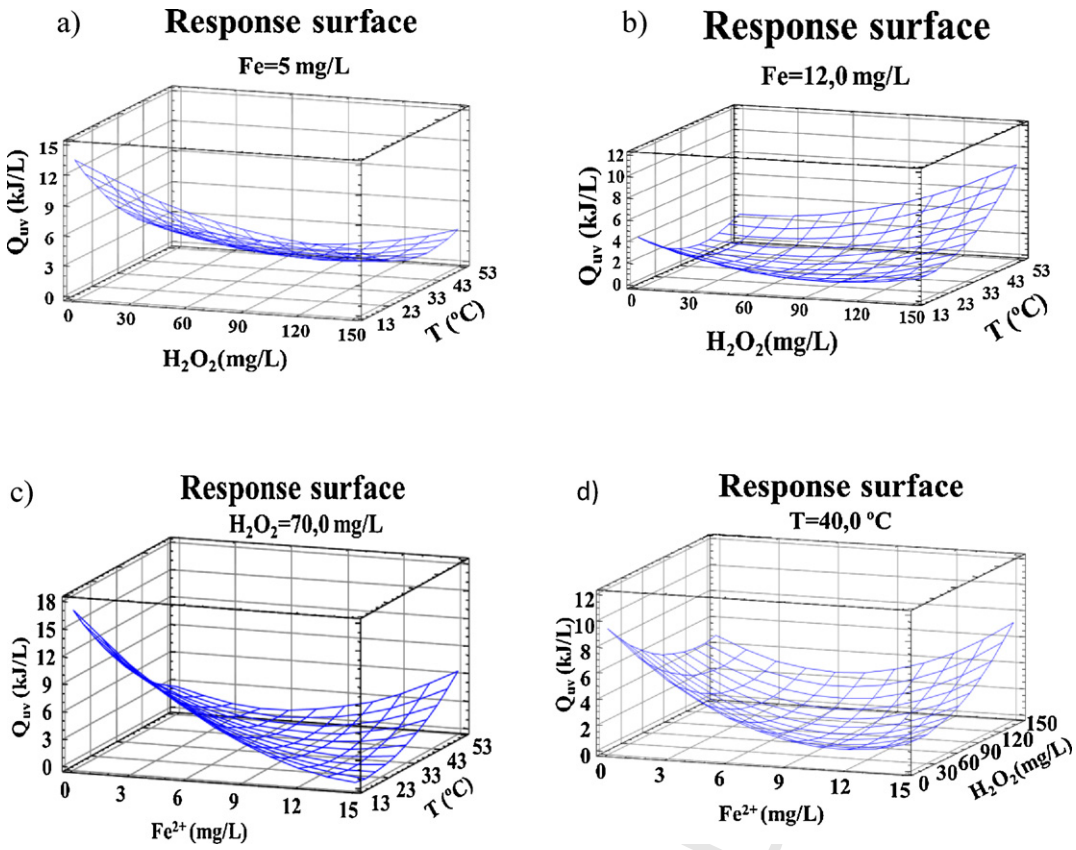

Fig. 3. Response surfaces for Q_{UV} versus (a) T and H_2O_2 concentration at 5 mg/L of Fe^{2+}, (b) T and H_2O_2 concentration at 12 mg/L of Fe^{2+}, (c) Fe^{2+} and T with H_2O_2 concentration constant at 70 mg/L, and (d) Fe^{2+} and H_2O_2 concentrations with T constant at 40 °C.

kept constant around its optimum according to Fig. 1(a) (around 70 mg/L). As expected, Q_{UV} decreased gradually with temperature up to an iron concentration of 8 mg/L. However, at higher iron concentrations, the effect on Q_{UV} with temperature increase is observed to be the contrary. This phenomenon, which reduces process efficiency, has previously been reported by other authors [26,34]. Furthermore, this effect is clearly demonstrated by comparing two of the experiments: during the experiment performed at 12 mg/L of Fe^{2+} and 70 mg/L of H_2O_2 at 20 °C, a 5% reduction in Fe^{2+} was observed after 40 min of treatment. However, in the experiment at the same Fe^{2+} and H_2O_2 concentrations, but at 40 °C, a 13% reduction in initial iron concentration was observed after the same reaction time. This loss of dissolved iron causes an increase in Q_{UV} ~~due to the decreased catalyst concentration, which~~ seems to be the experimental photo-Fenton parameter that most influences Q_{UV}.

Fig. 3(d) presents the effect of hydrogen peroxide and iron concentrations on Q_{UV} at a constant temperature of 40 °C. Q_{UV} was lower at low Fe^{2+} concentrations when the H_2O_2 concentration was increased. Once again optimal Fe^{2+} is observed at 40 °C (around 10 mg/L) across the whole range of hydrogen peroxide concentrations evaluated. However, it is clear that Q_{UV} falls when H_2O_2 is increased up to around 70 mg/L, which can be also observed in Figs. 1(a) and 3(b). This confirms reaction efficiency performance according to hydrogen peroxide concentration as already studied in photo-Fenton treatment of industrial wastewater. Neither a hydrogen peroxide concentration that is too low is desirable, because it slows down the Fenton reaction rate, nor should it be too high, because H_2O_2 competes successfully for hydroxyl radicals (~~reaction (4)~~) and decomposes without oxidizing the pollutants (~~reaction (5)~~) [20].

3.2. Optimal operating conditions experiment

The fit to this experimental design model by Statgraphics software made it possible to find the three optimal operating parameters, iron and hydrogen peroxide concentration, and temperature, within the ranges studied. Fig. 4 plots the contour diagram of the response surface model versus H_2O_2 and T, with Fe^{2+} constant at 10 mg/L. The minimum contour observed is 0.5 kJ/L, and as discussed above, the optimal area avoids high temperatures and high H_2O_2 concentrations.

A minimum of 0.4 kJ/L was required to minimize the accumulated energy needed for the removal of 95% of the contaminants added to the real MWTP effluents, and the corresponding optimal

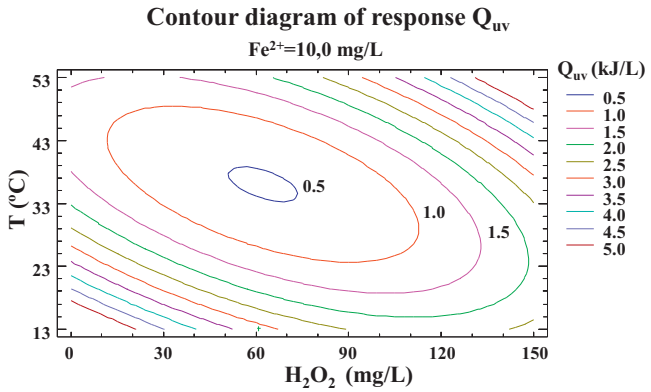

Fig. 4. Contour diagram of response surface model for H_2O_2 and T dependence.

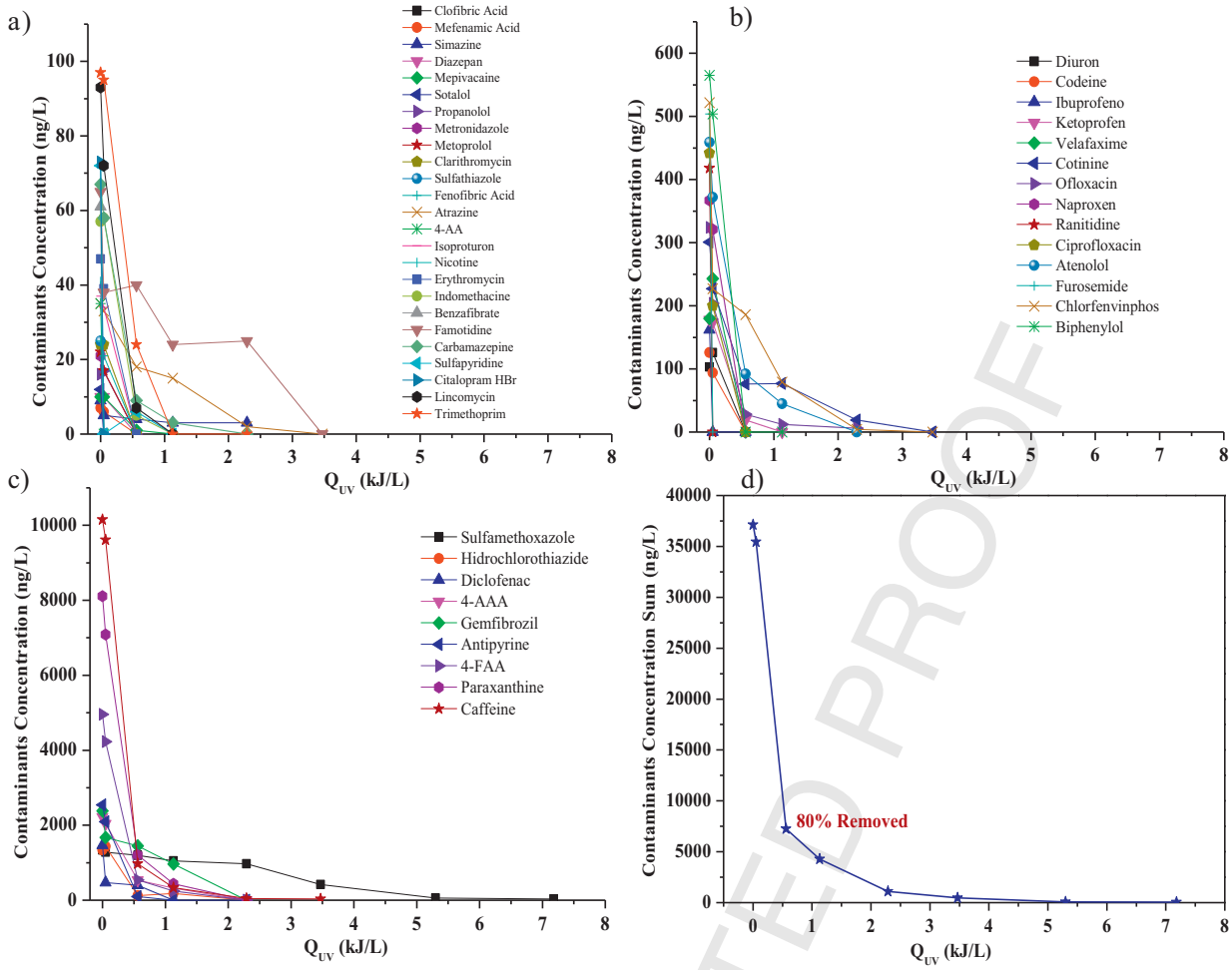

Fig. 5. Profile of photo-Fenton degradation of the contaminants found in MWTP effluent at concentrations ~~below~~ <100 ng/L ~~(a)~~, in the 100–1000 ng/L range ~~(b)~~, >1000 ng/L ~~(c)~~, and the sum of all contaminants found (d). ~~Conditions:~~ 9.7 mg/L ~~Fe~~ 68 mg/L H_2O_2, 34 °C.

experimental conditions for attaining this minimum Q_{UV} are: 10.16 mg/L of Fe^{2+}, 69.07 mg/L of H_2O_2, and 32.27 °C.

The last step of this study applied the above optimal operating conditions for minimizing Q_{UV} to eliminate the ~~microcontaminants~~ actually present in real MWTP effluent, resulting in over 99% degradation in only a few minutes of irradiation. Degradation of the ~~micropollutants~~ detected was monitored by LC–MS with the results presented in Fig. 5. 47 contaminants were found and quantified. Of these, a group of nine, Dipirone metabolites (4-AAA and 4-FAA), caffeine and its metabolite (paraxanthine), and some pharmaceuticals (hidroclorothiazide, sulfamethoxazole, gemfibrozil, diclofenac, and antipyrine), were the highest ~~with~~ concentrations over 1 μg/L (Fig. 5(c)).

The total pollutant load was around 38,000 ng/L. The degradation of the sum of micro-pollutants is plotted in Fig. 5(d). It can be observed that 84% of degradation was already attained only with 15 mg/L of H_2O_2 and an accumulated energy of 0.56 kJ/L, and finally, micro-contaminant removal was complete after 4 kJ/L.

4. Conclusions

A Solar photo-Fenton tertiary treatment for MWTP effluents containing emerging contaminants and other micro-pollutants was optimized using a three-level factorial experimental design. The results demonstrated that iron concentration, temperature, and their interaction are the parameters that most influence the accumulated energy necessary to remove over 95% of the micro-contaminants added to real MWTP effluents.

In conclusion, Fe^{2+} concentrations of around 10 mg/L and temperatures under 35 °C should be considered optimal for this type of tertiary treatment. Furthermore, it is important to highlight that high initial dosages of hydrogen peroxide are detrimental to accumulated energy. In fact, H_2O_2 concentrations over 70 mg/L should be avoided as inefficient, decreasing process efficiency. Finally, the optimal operating conditions found were tested on a real MWTP effluent, leading to ~~an 80%~~ reduction of micro-contaminants detected after 0.56 kJ/L of Q_{UV} and complete removal after less than 4 kJ/L. Therefore, solar photo-Fenton must be considered as an available effective technique for the tertiary treatment of MWTP effluents.

Acknowledgements

The authors wish to thank the European Commission for FEDER funding of the RITECA II Project (0401_RITECA_II_4_E) under "Competitiveness and Employment Promotion". The assistance of Mr. Agustín Carrión with the pilot plant reactor is gratefully acknowledged. Lucía Prieto-Rodríguez would like to thank the University of Almeria and CIEMAT-PSA for her Ph.D. research grant.

References

[1] EC, Directive of the European Parliament and of the Council 2000/60/EC Establishing a Framework for Community Action in the Field of Water Policy, Official Journal, C513, 23/10/2000, 2000.
[2] M. Schriks, M.B. Heringa, M.M.E. van der Kooi, P. de Voogt, A.P. van Wezel, Water Research 44 (2) (2009) 461–476.
[3] C.G. Daughton, T.A. Ternes, Environmental Health Perspectives 107 (1999) 907–938.
[4] D. Fatta-Kassinos, S. Meric, A. Nikolaou, Analytical and Bioanalytical Chemistry 399 (1) (2011) 251–275.
[5] M. Auriol, Y. Filali-Meknassi, R.D. Tyagi, C.D. Adams, R.Y. Surampalli, Process Biochemistry 41 (2006) 525–539.
[6] M.J. Gómez, M.J. Martínez Bueno, S. Lacorte, A.R. Fernández-Alba, A. Agüera, Chemosphere 66 (2007) 993–1002.
[7] M. Klavarioti, D. Mantzavinos, D. Kassinos, Environment International 35 (2009) 402–417.
[8] M. Petrovic, S. Gonzalez, D. Barceloï, Trends in Analytical Chemistry 22 (2003) 685–696.
[9] A. Jelic, M. Gros, A. Ginebreda, R. Cespedes-Sanchez, F. Ventura, M. Petrovic, D. Barceló, Water Research 45 (2011) 1165–1176.
[10] P.-D. Hansen, Trends in Analytical Chemistry 26 (11) (2007).
[11] A. Pal, K. Yew-Hoong Gin, A. Yu-Chen Lin, Science of the Total Environment 408 (2010) 6062–6069.
[12] J. Arana, J.A. Herrera Melian, J.M. Dona Rodriguez, O. Gonzalez Diaz, A. Viera, J. Perez Pena, P.M. Marrero Sosa, V. Espino Jimenez, Catalysis Today 76 (2002) 279–289.
[13] N.M. Al-Bastaki, Chemical Engineering and Processing 43 (2004) 935–940.
[14] K. Chiang, T.M. Lim, L. Tsen, C.C. Lee, Applied Catalysis A 261 (2004) 225–237.
[15] N. Nakada, H. Shinohara, A. Murata, K. Kiri, S. Managaki, N. Sato, Water Research 41 (2007) 4373–4382.
[16] R. Rosal, A. Rodríguez, J.A. Perdigón-Melón, M. Mezcua, M.D. Hernando, P. Letón, E. García-Calvo, A. Agüera, A.R. Fernández-Alba, Water Research 42 (2008) 3719–3728.
[17] E.C. Wert, F.L. Rosario-Ortiz, S.A. Snyder, Water Research 43 (2009) 1005–1014.
[18] M.A. Abu-Hassan, J.K. Kim, I.S. Metcalfe, D. Matzavinos, Chemosphere 62 (2006) 749–755.
[19] Y. Jiang, Ch. Petrier, T.D. Waite, Ultrasonics Sonochemistry 13 (2006) 415–422.
[20] S. Malato, P. Fernández-Ibáñez, M.I. Maldonado, J. Blanco, W. Gernjak, Catalysis Today 147 (2009) 1–59.
[21] A. Bernabeua, R.F. Verchera, L. Santos-Juanesa, P.J. Simónb, C. Lardínb, M.A. Martínezc, J.A. Vicentec, R. Gonzálezc, C. Llosác, A. Arquesa, A.M. Amat, Catalysis Today 161 (2011) 235–240.
[22] N. Klamerth, S. Malato, M.I. Maldonado, A. Agüera, A.R. Fernandez-Alba, Environmental Science and Technology 44 (2010) 1792–1798.
[23] J.J. Pignatello, E. Oliveros, A. MacKay, Critical Reviews in Environment Science and Technology 36 (2006) 1–84.
[24] I. Muñoz, J. Peral, J.A. Ayllón, S. Malato, M.J. Martin, J.-Y. Perrot, M. Vincent, X. Domènech, Environmental Engineering Science 24 (2007) 638–651.
[25] W. Gernjak, M. Fuerhacker, P. Fernandez-Ibañez, J. Blanco, S. Malato, Applied Catalysis B: Environmental 64 (2006) 121–130.
[26] A. Zapata, I. Oller, L. Rizzo, S. Hilgert, M.I. Maldonado, J.A. Sanchez-Perez, S. Malato, Applied Catalysis B: Environmental 97 (2010) 292–298.
[27] F. Ay, E.C. Catalkaya, F. Kargi, Journal of Hazardous Materials 162 (2009) 230–236.
[28] A.G. Trovó, T.F.S. Silva, O. Gomes Jr., A.E.H. Machado, W.B. Neto, P.S. Muller Jr., D. Daniel, Chemosphere 90 (2013) 170–175.
[29] N. Klamerth, S. Malato, A. Agüera, A. Fernandez-Alba, G. Maihot, Environmental Science and Technology 46 (2012) 2885–2892.
[30] M.J. Martínez-Bueno, A. Agüera, M.J. Gomez, M.D. Hernando, J.F. García-Reyes, A.R. Fernandez-Alba, Analytical Chemistry 79 (2007) 9372–9384.
[31] M.I. Maldonado, P.C. Passarinho, I. Oller, W. Gernjak, P. Fernández, J. Blanco, S. Malato, Journal of Photochemistry and Photobiology A: Chemistry 185 (2007) 354–363.
[32] R. Mostero, P. Ormad, E. Mozas, J. Sarasa, J.L. Ovelleiro, Water Research 40 (2006) 1561–1568.
[33] Design and Analysis of Experiments/Douglas C. Montgomery 5th Ed.
[34] T. Grundl, J. Delwiche, Journal of Contaminant Hydrology 14 (1993) 71–97.

Please cite this article in press as: L. Prieto-Rodríguez, et al., Solar photo-fenton optimization for the treatment of MWTP effluents containing emerging contaminants, Catal. Today (2013), http://dx.doi.org/10.1016/j.cattod.2013.01.002